# Journal Name

## ARTICLE TYPE

# Wavelet analysis and HHG in nanorings: their applications in logic gates and memory mass devices

Dario Cricchio,[*a] Emilio Fiordilino,[a]

We study the application of one nanoring driven by a laser field in different states of polarization in logic circuits. In particular we show that assigning boolean values to different state of the incident laser field and to the emitted signals, we can create logic gates such as OR, XOR and AND. We also show the possibility to make logic circuits such as half-adder and full-adder using one and two nanoring respectively. Using two nanorings we made the Toffoli gate. Finally we use the final angular momentum acquired by the electron to store information and hence show the possibility to use an array of nanorings as a mass memory device.

## 1 Introduction

The rapid development of the nanosciences opens new technological frontiers. Computer science is one of them. In fact by some years we are observing a saturation in the microprocessors performance which requires the finding of new objects that allow the construction of logic circuits faster and smaller than today's. However, today's technology combines electronics and optics. This combination limits the speed input/output transmission; hence is important to create entirely optical devices. The importance of using only optical devices is due to the much faster data transmission and to the lower energy consumption than when using traditional devices.[1]. For these reasons the research is focusing on a new kind of devices that show electrical and optical properties and that can be suitable to construct logic circuits: nanorings and graphenes are an example of them. They show interesting behavior in nanotechnology, optic and computer science thanks to their electrical and optical properties that make them apt to implementation in logic circuits. One important property of the graphene is its dispersion relation. In fact it is linear around the six corners of the hexagonal pattern leading to the vanishing of the effective mass of electrons and holes[2]. Another noteworthy object is the nanoring, a planar structure with a ring geometry. Gold nanoring arrays are studied for biosensing applications in the fiber-optic communication window[3]. The interaction between a strong laser field and molecules give the possibility to observe non linear processes that cannot be described by the standard perturbation theory[4].

Analytic and experimental studies on mesoscopic molecules

show that the large size and polarizability make them interesting sources of harmonics[5–9]. Nanorings present several optical properties, in particular they show that the high harmonic generation spectrum (HHG), obtained when they are driven by a circularly polarized laser field, is more intense than the HHG spectrum obtained from benzene[10]. Moreover nanorings driven by a two color laser field can efficiently emit a broad harmonic spectrum; and it has been shown the possibility of controlling the polarization of the emitted harmonics by changing the laser parameters and also to have a final angular momentum of the electron in the nanoring[11–13]. It is also numerically demonstrated that ring current initial states generate a nonstandard ionization and harmonic generation by strong laser pulses and that the internal state is transferred to the tunneling wave packets, which receive an initial momentum[14].

A circularly polarized ultraviolet laser pulse excites a unidirectional valence-type electronic ring current in an oriented molecule. The net ring current generated by the laser pulse is about $84.5\ \mu$A and could be induced by means of permanent magnetic fields[15]. Magnetic fields can also induced by a circular polarized laser pulse[16].

The aromatic group, containing six carbon atoms, can be considered as the nanoring with the smallest radius. It corresponds to a single cell of graphene. Nanorings with large radius are obtained joining strips of graphene[17], by self-assembling RNA nanorings based on RNAI/IIi kissing complexes[18] or by an array of nano apertures[19]. A mesoscopic ring, treated with a magnetic flux, is used to make NAND gate[20], where the ring is attached symmetrically to two metallic electrodes and two gate voltages are applied in one arm of the ring, these are treated as the two inputs of the NAND gate. Optical signals are used in[21] where two silicon microring resonators are used to perform XOR and XNOR operations. In[22] it is shown the possibility to generate

*dario.cricchio@unipa.it
[a]Dipartimento di Fisica e Chimica, Università di Palermo, Via Archirafi 36, 90123 Palermo (Italy)
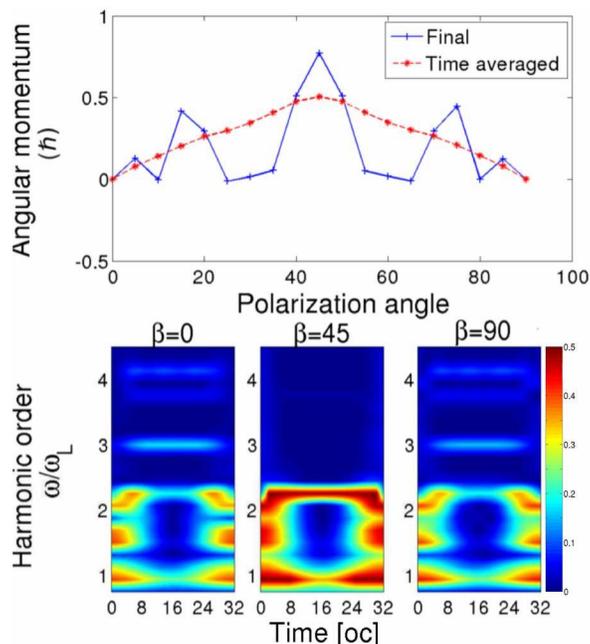
**Fig. 1** Top: Final (solid line) and time averaged (dashed line) angular momentum obtained with $\hbar\omega_L = 2$ eV and $I_L = 10^{14}$ W/cm$^2$ and R=2.7 $a_0$. Bottom: Morlet wavelet analysis of the dipole moment for $\beta = 0°, 45°, 90°$.



**Fig. 2** Final (solid line) and time averaged (dashed line) angular momentum obtained with $\hbar\omega_L = 2$ eV and $I_L = 10^{14}$ W/cm$^2$ and R=2.7 $a_0$. Initial angular momentum $L < 0$ (top) and $L > 0$ (bottom).

optical NOT and XOR logic operation based on terahertz optical asymmetric demultiplexer. Also thermal logic gates exist that can do simple calculations using the phonons as information[23]. The symmetry of the wave packets and their shape are used like quantum bits[24]. XOR and XNOR operationswere simultaneously implemented using an electro-optic directed logic circuit based on two cascaded silicon microring resonators modulated through the plasma dispersion effect[25]. Using two parallel microring resonators it is possible fabricate direct logic circuits that perform the operations: OR/NOR, AND/NAND[26,27]. The realizations of nanoscale integrated all-optical XNOR, XOR, NOT, and OR logic gates using plasmonic slot waveguides based on linear interference between surface plasmon polariton modes is reported in[28]. In[29–34] gate response in a double quantum ring, where each ring is threaded by a magnetic flux, is investigated . With their model the authors have designed a AND, OR, NOR and XOR gate using mesoscopic rings, based on the effect of quantum interference. The importance of that work is the simplicity of the geometry and the smallness of the dimension. Logic circuits with field-effect transistors based on single carbon nanotubes are reported in[35]. These devices feature local gates that provide excellent capacitive coupling between the gate and nanotube. The transistors show favourable device characteristics such as high gain, large on-off ratio, and room-temperature operation.

This paper deals with the possibility of using nanorings, driven by a laser field, as logical gates. Our system is composed by one nanoring, with only one active electron, driven by an elliptically polarized laser field[4]. We calculate the harmonics and the Raman lines emitted and the angular momentum acquired by the electron in different states of polarization of the incident laser
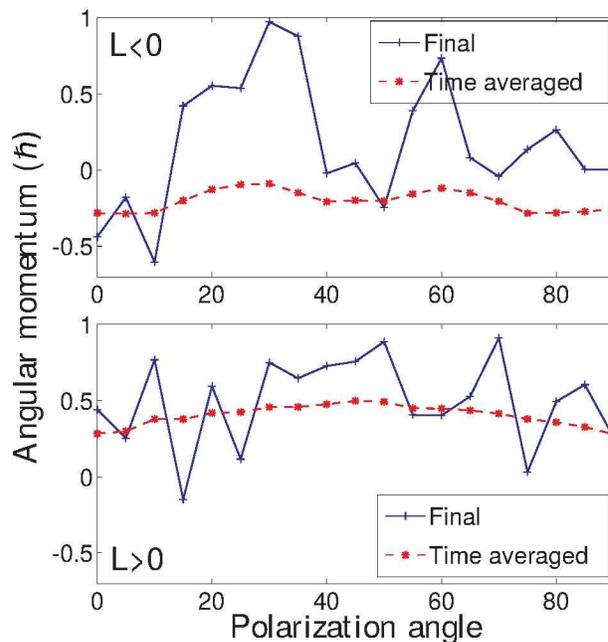
field. The process that we use in this work is the high harmonic generation (HHG)[36]. Using a nanoring instead of larger structure is due to the fact that the computer devices require an increasing of the miniaturization in order to obtain lower power consumption and lower path between the other components. In[37] it is demonstrate as the harmonic spectrum of one nanoring with a radius of 2.7 $a_0$ is compatible with the spectrum of the graphene plasma. The HHG spectrum is generated by a non-linearity of the electron-laser interaction energy that forces the system to emit a spectrum of harmonics of the laser field[38,39]. Several studies shows that the use of a two-color laser field or of a laser photon energy resonant between the ground state and the first excited state can enhance the emitted spectrum[40–43]. Then we calculate the HHG spectra and, from the use of the wavelet transform, we recognize the presence of a signal composed by the first two harmonics and the Raman lines. We perform our calculations by varying the states of polarization of the incident laser field. We also calculate the angular momentum acquired by the electron in order to use it to create a truth table of logical operations and then to use the nanoring as a logic gate. In[44] it is demonstrated a direct optical half-adder based on cascaded microring resonators. the authors implement the addition of two bits obtaining the Sum and Carry of the addition at their output ports simultaneously. Another interesting way of implementation of logic circuits is the molecular logic, where many of the simpler logic operations can be identified within chemical reactions[45]. Photonic logic gate was demonstrated in DNA-Based devices where the DNA is capable of AND, NAND, and INHIBIT logic operation[46]. The goal of this work is to introduce a new logic device based on nanorings. We demonstrate how the nanoring can be used to construct logic gates, in particular the AND, OR, and XOR logic gates. These

Nanoscale Accepted Manuscript
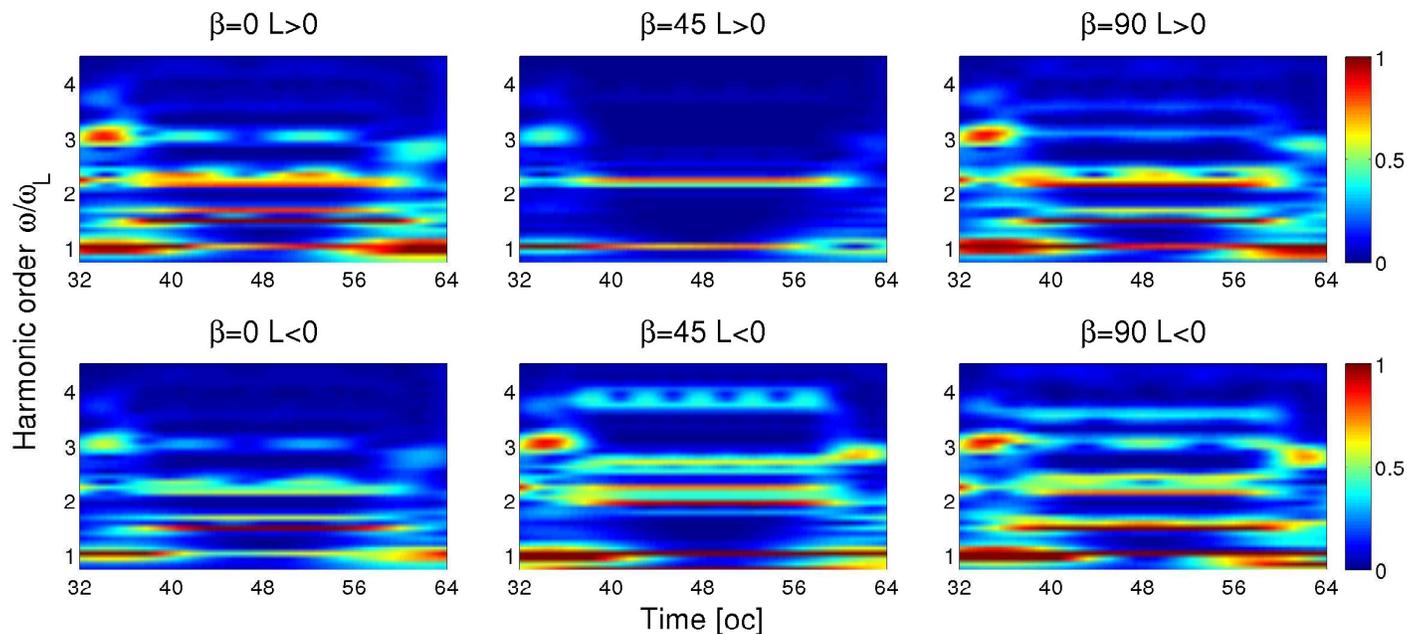
**Fig. 3** Morlet wavelet analysis of the dipole moment with $\hbar\omega_L = 2$ eV and $I_L = 10^{14}$ W/cm$^2$ and R=2.7 $a_0$ for $\beta = 0°, 45°, 90°$ and an initial angular momentum $L > 0$ (top line) and $L < 0$ (bottom line).

| $\mathscr{E}_{x,y}$ | $H_I$ | $H_{II}$ | $H_{R1}$ | $H_{R2}$ | $L_z$ |
|---|---|---|---|---|---|
| 0 0 | 0 | 0 | 0 | 0 | 0 |
| 1 0 | 1 | 1 | 1 | 1 | 0 |
| 0 1 | 1 | 1 | 1 | 1 | 0 |
| 1 1 | 1 | 0 | 1 | 0 | 1 |
| $L=0$ | OR | XOR | OR | XOR | AND |

**Table 1** Truth table: in input we have the laser states $\mathscr{E}_{x,y}$ and in output we have the first two odd harmonics, the Raman transitions and the final angular momentum.

| $\mathscr{E}_{x,y}$ | $H_1$ | $H_{II}$ | $H_{R1}$ | $H_{R2}$ | $L_z$ |
|---|---|---|---|---|---|
| 0 0 | 1 | 0 | 1 | 0 | 1 |
| 1 0 | 1 | 1 | 1 | 0 | 1 |
| 0 1 | 1 | 1 | 1 | 0 | 1 |
| 1 1 | 1 | 0 | 1 | 0 | 1 |
| $L>0$ | BUFFER | XOR | BUFFER | RESET | BUFFER |

| $\mathscr{E}_{x,y}$ | $H_1$ | $H_{II}$ | $H_{R1}$ | $H_{R2}$ | $L_z$ |
|---|---|---|---|---|---|
| 0 0 | 1 | 0 | 1 | 0 | 1 |
| 1 0 | 1 | 1 | 1 | 0 | 1 |
| 0 1 | 1 | 1 | 1 | 0 | 0 |
| 1 1 | 1 | 1 | 1 | 1 | 0 |
| $L<0$ | BUFFER | OR | BUFFER | AND | // |

**Table 2** Truth table: in input we have the laser states $\mathscr{E}_{x,y}$ with a initial positive angular momentum (top) and with a negative initial angular momentum (bottom). In output we have the first two odd harmonics, the Raman transitions and the final angular momentum.

logic gates permit to construct the universal reversible Toffoli and Fredkin gates, hence the possibility to construct any logic circuit. We give examples of implementation of nanoring to construct a basic logic circuit such as the half and the full-adder and finally we discuss the possibility of constructing a memory mass device using an array of nanorings.

## 2 Theory

In our system we consider one nanoring of radius $R$ in the single active electron approximation driven by one laser elliptically polarized along the same plane. The equation of the electric field is:

$$\vec{\mathscr{E}}_L(t) = \mathscr{E}_0 f(t) \big[ \hat{\varepsilon}_x \cos(\beta) \cos(\omega_L t) +$$
$$+ \hat{\varepsilon}_y \sin(\beta) \sin(\omega_L t) \big] \quad (1)$$

where $f(t)$ is the pulse shape, $\hat{\varepsilon}_x$ and $\hat{\varepsilon}_y$ are the unit vectors along the $x$ and $y$ axes respectively, $\omega_L$ is the angular frequency of the external laser field and $\beta$ is a parameter that characterize the polarization of the electric field. In particular for $\beta = 0°$ we have a laser polarized along the $x$ axis, for $\beta = 90°$ we have a laser

polarized along the $y$ axis and for $\beta = 45°$ we have a circular polarized laser. In dipole approximation and within the single active electron approximation, the Hamiltonian of the system is[4,47]

$$\mathscr{H} = \frac{\hbar^2 \ell_z^2}{2m_e R^2} + e\mathscr{E}_0 R f(t) \Big[ \cos(\beta) \cos(\omega_L t) \cos(\varphi) +$$
$$+ \sin(\beta) \sin(\omega_L t) \sin(\varphi) \Big], \quad (2)$$

where $\ell_z$ is the $z$ component of the orbital angular momentum operator (in units of $\hbar$), whose eigenvectors and eigenvalues are the angular momentum states $\ell_z \mid m\rangle = m \mid m\rangle$ with $m = 0, \pm 1, \ldots,$ and $m_e$ is the electron mass[48]. Solving the time dependent Schrödinger equation of the system, we find the expansion co-
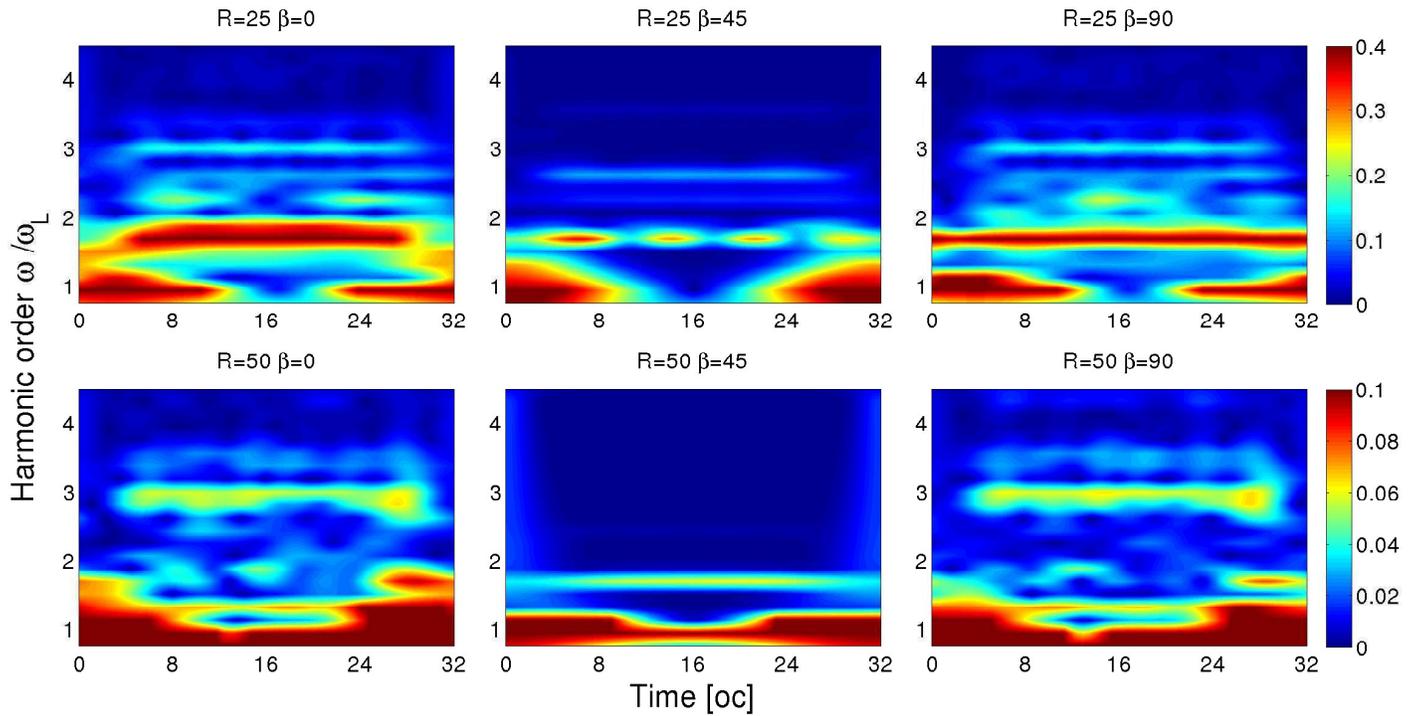
**Fig. 4** Morlet wavelet analysis of the dipole moment for $\beta = 0°, 45°, 90°$, a radius of $R = 25$ (top line) and $R = 50$ $a_0$ (bottom line), a energy of laser photon of 0.1 eV and an intensity of $10^{10}$ W/cm$^2$.

efficient $a_m$ of the wave function $|t\rangle$:

$$|t\rangle = \sum_{m=-\infty}^{+\infty} a_m(t) |m\rangle \tag{3}$$

where $|m\rangle$ are eigenstates of the free Hamiltonian with energy

$$\hbar\omega_m = \frac{\hbar^2}{2m_e R^2} m^2. \tag{4}$$

| $\mathscr{E}_{x,y}$ | Sum | Carry |
|---|---|---|
| 0 0 | 0 | 0 |
| 1 0 | 1 | 0 |
| 0 1 | 1 | 0 |
| 1 1 | 0 | 1 |

**Table 3** Truth table of the half adder: in input we have the laser states $\mathscr{E}_{x,y}$ and in output we have the values of the second odd harmonic and the $H_{R2}$ line for the sum, and the values of $L_z$ for the carry.

From the state $|t\rangle$ we can calculate the dipole moment of the system as:

$$\vec{\mathscr{D}} = e\vec{r}(t) = \hat{\varepsilon}_x \langle t | x | t\rangle + \hat{\varepsilon}_y \langle t | y | t\rangle =$$

$$= \sum_{m=-\infty}^{+\infty} \left[ \hat{\varepsilon}_x \Re\left(a_{m-1}^* a_m\right) + \hat{\varepsilon}_y \Im\left(a_m^* a_{m-1}\right) \right] \tag{5}$$

where $\vec{r}$ is the position of the electron. The angular momentum acquired by the electron is:

$$L_z(t) = \sum_{m=-\infty}^{+\infty} |a_m(t)|^2 \hbar m, \tag{6}$$

and the correspondent time averaged angular momentum is:

$$\langle L_z \rangle = \frac{1}{T} \int_0^T L_z(t) \mathbf{d}t. \tag{7}$$

From the angular momentum we can define the magnetic momentum as $\vec{m} = \gamma \vec{L}$, with $\gamma$ the gyromagnetic ratio of the electron[49].

## 3   Results

In our calculations we use different configurations of laser intensity and laser photon energy. In particular we use laser intensities $I_L$ in the range $10^{10} - 10^{14}$ W/cm$^2$ and laser photon energy $\hbar\omega_L$ in the range $0.1 - 2$ eV (12398 and 620 nm) and a radius between $R = 2.7$ $a_0$, like the radius of the aromatic group, and $R = 100$ $a_0$. In fact large values of radius require small energies of the laser photon and less laser intensity. Then the dependence upon the radius permits to engineer the nanoring to obtain particular transition energies and to make it flexible for various uses. In Fig. 1 (top) we show the final and the time averaged angular momentum versus the polarization angle with R=2.7 $a_0$, $\hbar\omega_L = 2$ eV and $I_L = 10^{14}$ W/cm$^2$. The time averaged angular momentum is calculated for each polarization angle using Eq. 7. In this simulation we use a laser duration of 32 optical cycles (oc) with a trapezoidal pulse shape. To understand when a signal is present, we performed a Morlet wavelet analysis on the total spectrum. The

Morlet mother wavelet is defined as:

$$M(x) = \left(e^{-ix} - e^{-\frac{\sigma_0^2}{2}}\right) e^{-\frac{x^2}{2\sigma_0^2}} \tag{8}$$

where $\sigma_0$ is a parameter that indicates the time-frequency resolution of the integration[50]. In our calculation, we chose $\sigma_0 = 6$, that correspond to 6 oscillations of the signal within the Morlet wavelet shape. We indicate with $H_1$ and $H_{II}$, the first two odd harmonics of the spectrum and with $H_{R1}$ and $H_{R2}$ the signals corresponding to the Raman transitions located near the first and the second even harmonics of the HHG spectrum[51]. In fact from Eq. 4 we have $\hbar\omega_1 = 1.9$ eV, $\hbar\omega_2 = 7.6$ eV, $\hbar\omega_3 = 17$ eV, then we can define the signal $H_{R1}$ as the transition between the virtual level with energy of $2\hbar\omega_1 = 3.8$ eV and the ground state, and the signal $H_{R2}$ as the combination of two Raman transition: $\hbar\omega_2$ and $\hbar\omega_2 + \hbar\omega_1 = 9.4$ eV. The photon energy Raman transitions depend upon the radius of the nanoring, we chose the value R=2.7 $a_0$ in order make the system comparable to a single cell of graphene or an aromatic group.

In Fig. 1 (bottom) we show the wavelet analysis for $\beta = 0°, 45°, 90°$. In this analysis the line $H_{R1}$ is slightly shifted up the 4 eV by the presence of a non Raman line. In fact if within the oscillations in $\sigma_0$ we have several lines, the final value of the wavelet is shifted towards the more intense line. Now we create a truth table where we associate the values 1 and 0 to the polarization states of the incident laser field and to the presence or absence of signals. In particular we can divide the elliptical polarized laser into two components: $\mathscr{E}_x$ parallel to the $x$ axis and $\mathscr{E}_y$ parallel to the $y$ axis. When the laser is off, we have the state $\mathscr{E}_x = 0$ and $\mathscr{E}_y = 0$ ($\mathscr{E}_{x,y} = (0,0)$); for $\beta = 0° \rightarrow \mathscr{E}_{x,y} = (1,0)$, for $\beta = 90° \rightarrow \mathscr{E}_{x,y} = (0,1)$ and for $\beta = 45° \rightarrow \mathscr{E}_{x,y} = (1,1)$. We also associate the value 1 when the system presents a final angular momentum $L_z$. In Tab. 1 we can see that the first odd harmonic and the $H_{R1}$ line behave as a OR logic gate, the second odd harmonic and the $H_{R2}$ line behaves as a XOR logic gate and $L_z$ behave as a AND logic gate. Now we study the system using two consecutive laser pulses. We use the first laser pulse, circularly polarized, as a pump ($\beta = 45°$) and the second laser pulse, elliptically polarized, to probe the system. We make this choice in order to prepare the system with an initial angular momentum. From the dashed line of Fig. 1 we can see that for $\beta = 45°$ we have a positive time averaged angular momentum and the emission of the first odd harmonic and the $H_{R1}$ line (Fig. 1 (bottom-center)). We obtain different results varying the sign of the initial angular momentum. In Fig. 2 we show the final and the time averaged angular momentum with different signs of the initial angular momentum: $L < 0$ (top) and $L > 0$ (bottom). In this simulation we used a laser duration of 64 oc where in the first 32 oc we prepared the system with an initial angular momentum in order to study the nanoring with different starting conditions. We used a trapezoidal laser shape with 2 oc of ascent and descent laser. In Fig. 3 we show the respective wavelet analysis. If we have a positive initial angular momentum we obtain a BUFFER for the first odd harmonic, the $H_{R1}$ line, and for the final angular momentum, a XOR logic gate for the second odd harmonic and a RESET for the $H_{R2}$ line; if the initial angular momentum is nega-

tive, we obtain a BUFFER for the first odd harmonic and the $H_{R1}$ line, an AND logic gate for the $H_{R2}$ line and an OR for the second odd harmonic. These results are listed in the truth table of Tab. 2.

We also decrease the laser intensity and the energy of the photon laser and increase the radius up to 100 $a_0$. In fact with large radii we obtain the same results but using a laser intensity of $10^{10}$ W/cm$^2$ and a laser photon of 0.1 eV. These new parameters are preferable for the constructions of logic port because for manufacturing purposes. In Fig. 4 we show the wavelet transform using a radius of $R = 25$ and $R = 50$ $a_0$ respectively, a laser intensity of $10^{10}$ W/cm$^2$ and a laser photon of 0.1 eV and without an initial angular momentum. We can see that the structure of the emitted lines is the same but less defined. This because the harmonic spectrum present several non Raman lines that shift and enlarge the lines.

Now we show how nanorings can be arranged to form logic circuits. Examples of logical circuits are the half and the full adder.

The half adder is a digital electronic component that has in input two bits ($\mathscr{E}_x$ and $\mathscr{E}_y$ in our case) and give in output their sum ($S$) and their carry ($C$). We can use the nanoring without initial angular momentum as an half adder using as output the second odd harmonic, the $H_{R2}$ line and $L_z$ (Tab. 3). Combining two nanorings, we have the possibility to make a full adder, where we use the carry of a previous summation. In fact we can use the harmonics obtained by one nanoring as input for a second nanoring et cetera. In this way we obtain a logic circuit with a set of concatenated nanorings. The presence of XOR and AND logic gates give us the possibility to make a Toffoli gate. The Toffoli gate is an universal reversible logic gate that permits to construct any reversible circuit. It has 3 bit inputs ($a, b$ and $c$) and outputs and realizes the function $c$ XOR ($a$ AND $b$). In fact if we set the first two bits, the Toffoli gate inverts the third bit, otherwise all bits remain unchanged. Then it is possible to use the nanorings as a Toffoli gate and create any logic circuit. Moreover, XOR and AND logic gates permit us to construct the Fredkin gate (controlled-SWAP). This gate is important for the reversible computing, in fact this is a three-bit gate that swaps the values of the second and third bits if the first bit is set to 1.

We now suggested a way of using the nanoring to store information. When a nanoring is driven by a circular polarized laser field, the electron will round on it with a circular motion. This movement will generate a current $I$. If we call $\vec{S}$ the surface of the nanoring, the magnetic moment generated by the motion of the electron will be:

$$\vec{m} = I \int d\vec{S}, \tag{9}$$

or, in terms of the angular momentum: $\vec{m} = \gamma\vec{L}$. If we have a planar array of nanorings and if $\vec{\sigma}$ is the surface of the laser spot containing several nanorings, the magnetic momentum generated will be proportionally to the summation of the the contributions of each nanoring within the laser spot surface (Fig. 5). Then we can use the nanoring to store information with the magnetic momentum.

When the nanoring is driven by a laser field in the state (1,1), it acquire an angular momentum and we obtain $L_z = 1$. Then if

we use another laser pulses with inverse circular polarization, we obtain an angular momentum state $L_z = 0$; we can consider the angular momentum like a pseudo-spin.

These simple behaviours make the nanoring an interesting object to store information.

## 4 Conclusions

In this article we propose the nanorings as a real alternative to modern logic components thanks to their size and speed.

We investigated the possibility to use nanorings driven by a laser field to make logic circuits. In particular we used the emitted signals and the final angular momentum of the nanoring to create logic gate that can be used to make logic operations. In fact we noticed the possibility to construct the XOR, OR and AND logic gates and apply them to make a half and full adder. Combining two or more nanorings, we can obtain a full adder, but the presence of XOR and AND logic gates gives us the possibility to make the Toffoli and the Fredking gates. These are universal reversible logic gates that permit the construction of any reversible circuit. The Toffoli gate has 3 bit inputs ($a$, $b$ and $c$) and outputs and realizes the function $c$ XOR ($a$ AND $b$). The Fredking gate is a three-bit gate that swaps the values of the second and third bits if the first bit is set to 1. Then with these two universal reversible logic gates we can create any logic circuit.

We can use also the angular momentum acquired by the electron in the nanoring to store information. In fact we can consider the final angular momentum like a pseudo-spin that can be reversed by changing the direction of circular polarization of the incident laser field. Our all-optical system has the advantage that the entire process, including harmonics generation, Raman transitions, and angular momentum, takes about $10^{-15}$ seconds. In addition we can create cells of nanoring arrays and store informations on it using the laser to generate a magnetic moment. In this paper we showed several simulations to study the system with different parameters, such as the radius, the energy of the laser photon and the intensity of the laser. In fact if we enlarge the radius and decrease the energy of the laser photon, we obtain the same results. If we think to construct a nanoring with a radius of 25 or 50 $a_0$, we can use a laser photon with energy $\sim 0.1$ eV and a laser intensity of $\sim 10^{10}$ W/cm$^2$.

## 5 Acknowledgment

## References

1 S. Caulfield, H. J.and Dolev. *Nat Photon*, 4(5):261–263, May 2010.

2 P. R. Wallace. *Phys. Rev.*, 71:622–634, 1947.

3 H. Jiang, T. Li, J. Yang, Mittler. S., and J. Sabarinathan. *Nanotechnology*, 24(46):465502, 2013.

4 C. J. Joachain, N. J. Kylstra, and R. M. Potvliege. *Atoms in intense laser fields*. Cambridge University Press, 2012.

5 G. S. Voronov and N. B. Delone. *J. Exp. Theor. Phys. Lett.*, 1, 1965.
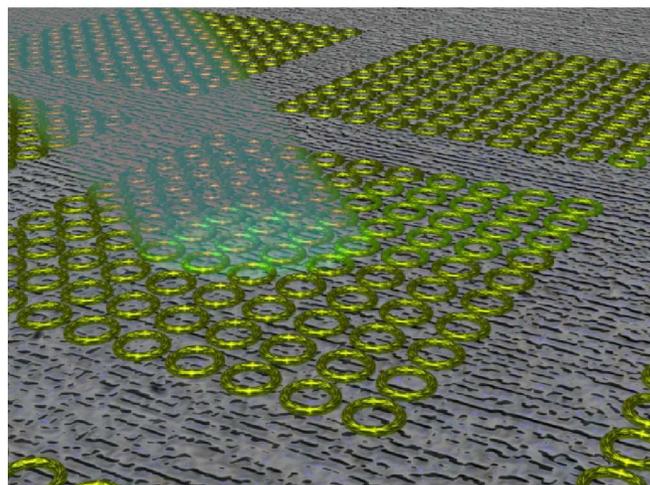
**Fig. 5** Schematic representation of array of nanorings used to store informations. When one array is driven by the laser field, it creates a magnetic moment that represents a bit.

6 O. E. Alon, V. Averbukh, and N. Moiseyev. *Phys. Rev. Lett.*, 80:3743–3746, 1998.

7 V. Averbukh, O. E. Alon, and N. Moiseyev. *Phys. Rev. A*, 64:033411, 2001.

8 P. Žd'ánská, V. Averbukh, and N. Moiseyev. *J. Chem. Phys.*, 118(19):8726–8738, 2003.

9 S. A. Sørngård, S. I. Simonsen, and J. P. Hansen. *Phys. Rev. A*, 87:053803, 2013.

10 I. Bâldea, A. K. Gupta, L. S. Cederbaum, and N. Moiseyev. *Phys. Rev. B*, 69:245311, 2004.

11 D. Cricchio and E. Fiordilino. *Las. Phys. Lett.*, 11(6):066002, 2014.

12 D. Cricchio, E. Fiordilino, and F. Persico. *Phys. Rev. A*, 86:013201, 2012.

13 G. Castiglia, P. P. Corso, D. Cricchio, R. Daniele, E. Fiordilino, F. Morales, and F. Persico. *Phys. Rev. A*, 88:033837, 2013.

14 X. Xie, A. Scrinzi, M. Wickenhauser, A. Baltuška, I. Barth, and M. Kitzler. *Phys. Rev. Lett.*, 101:033901, Jul 2008.

15 I. Barth, J. Manz, Y. Shigeta, and K. Yagi. *J. Am. Chem. Soc*, 128(21):7043–7049, 2006.

16 I. Barth and J. Manz. *Phys. Rev. A*, 75:012510, Jan 2007.

17 V. M. Fomin. *Physics of Quantum Rings*. NanoScience and Technology. Springer, 2013.

18 W. W. Grabow, P. Zakrevsky, K. A. Afonin, A. Chworos, B. A. Shapiro, and L. Jaeger. *Nano Lett.*, 11(2):878–887, 2011. PMID: 21229999.

19 A. Chovin, P. Garrigue, I. Manek-Hönninger, and N. Sojic. *Nano Lett.*, 4(10):1965–1968, 2004.

20 S.K. Maiti. *Phys. Scr.*, 80(5):055704, 2009.

21 L. Zhang, R. Ji, L. Jia, L. Yang, P. Zhou, Y. Tian, P. Chen, Y. Lu, Z. Jiang, and Y. Liu. *J. Phys: Conference Series*, 276(1):012105, 2011.

22 W. Ying, Z. Xin-Liang, and H. De-Xiu. *Ch. Phys.*, 13(6):882, 2004.

23 L. Wang and B. Li. *Phys. Rev. Lett.*, 99:177208, 2007.

24 E. A. Shapiro, M. Spanner, and M. Y. Ivanov. *Phys. Rev. Lett.*, 91:237901, 2003.

25 L. Zhang, J. Ding, Y. Tian, R. Ji, L. Yang, H. Chen, P. Zhou, Y. Lu, W. Zhu, and R. Min. *Opt. Express*, 20(11):11605–11614, May 2012.

26 Y. Tian, L. Zhang, and L. Yang. *Opt. Express*, 20(15):16794–16800, Jul 2012.

27 Y. Tian, L. Zhang, R. Ji, L. Yang, P. Zhou, H. Chen, J. Ding, W. Zhu, Y. Lu, L. Jia, Q. Fang, and M. Yu. *Opt. Lett.*, 36(9):1650–1652, May 2011.

28 Y. Fu, X. Hu, C. Lu, S. Yue, H. Yang, and Q. Gong. *Nano Letters*, 12(11):5784–5790, 2012. PMID: 23116455.

29 S. K. Maiti. *Physics Letters A*, 373(48):4470 – 4474, 2009.

30 S. K. Maiti. *Solid State Communi.*, 149(39-40):1684 – 1688, 2009.

31 S. K. Maiti. *Solid State Commun.*, 149(47-48):2146 – 2150, 2009.

32 S. K. Maiti. *Solid State Commun.*, 149(39-40):1623 – 1627, 2009.

33 S. K. Maiti. *Journal of the Physical Society of Japan*, 78(11):114602, 2009.

34 S. K. Maiti. *Physica Scripta*, 80(5):055704, 2009.

35 A. Bachtold, P. Hadley, T. Nakanishi, and C. Dekker. *Science*, 294(5545):1317–1320, 2001.

36 M. Ferray, A. L'Huillier, X. F. Li, L. A. Lompre, G. Mainfray, and C. Manus. *J. Phys. B: At. Mol. and Opt. Phys.*, 21(3):L31, 1988.

37 R. Ganeev, E. Fiordilino, D. Cricchio, Corso P., M. Suzuki, S. Yoneya, and H. Kuroda. Graphene in strong laser field: experiment and theory. *Las. Phys. Lett.*, 12:065401–, 2015.

38 A. Matos-Abiague and J. Berakdar. *Phys. Lett. A*, 330(1-2):113–119, 2004.

39 F. Blanchard, L. Razzari, H.C. Bandulet, G. Sharma, R. Morandotti, J. C. Kieffer, T. Ozaki, T. Reid, H. F. Tiedje, H. K. Haugen, and F. A. Hegmann. *Opt. Express*, 15(20):13212–13220, Oct 2007.

40 R. A. Ganeev, C. Hutchison, T. Witting, F. Frank, S. Weber, W. A. Okell, E. Fiordilino, D. Cricchio, F. Persico, A. Zaïr, et al. *J. Opt. Soc. Am. B*, 30(1):7–12, 2013.

41 R. A. Ganeev, P. A. Naik, H. Singhal, J. A. Chakera, M. Kumar, M. P. Joshi, A. K. Srivastava, and P. D. Gupta. *Phys. Rev. A*, 83:013820, 2011.

42 I. J. Kim, C. M. Kim, H. T. Kim, G. H. Lee, Y. S. Lee, J. Y. Park, D. J. Cho, and C. H. Nam. *Phys. Rev. Lett.*, 94:243901, 2005.

43 N. F. Hinsche, A. S. Moskalenko, and J. Berakdar. *Phys. Rev. A*, 79:023822, 2009.

44 Y. Tian, L. Yang, L. Zhang, R. Ji, J. Ding, P. Zhou, W. Zhu, and Y. Lu. *Phot. Tech. Lett., IEEE*, 24(8):643–645, April 2012.

45 S. de Silva, A. P.and Uchiyama. *Nat Nano*, 2(7):399–410, Jul 2007.

46 A. Saghatelian, N. H. Völcker, K. M. Guckian, V. S.-Y. Lin, and M. R. Ghadiri. *J. Am. Chem. Soc.*, 125(2):346–347, 2003. PMID: 12517142.

47 J. D. Jackson. *Classical Electrodynamics*. John Wiley et Sons Inc, 1998.

48 C. Cohen-Tannoudji, B. Diu, and F. Laloë. *Quantum mechanics*. John Wiley et Sons Inc, 1977.

49 L. D. Landau and E.M. Lifshitz. *Quantum Mechanics: Nonrelativistic Theory*. Butterworth Heinemann. Butterworth-Heinemann, 1977.

50 S. De Luca and E. Fiordilino. *J. Mod. Opt.*, 45(9):1775–1783, 1998.

51 B. H. Bransden and C. J. Joachain. *Physics of Atoms and Molecules*. Pearson Education. Prentice Hall, 2003.